

Bi₂MTaO₇ (M = Al, Fe, Ga, In) PHOTOCATALYST FOR ORGANIC COMPOUNDS DEGRADATION UNDER UV AND VISIBLE LIGHT

LETICIA M. TORRES-MARTINEZ^{1*}, ISAIAS JUAREZ-RAMIREZ¹, JUAN S. RAMOS-GARZA¹, FRANCISCO VAZQUEZ-ACOSTA¹, AND SOO WOHN LEE²

¹Departamento de Ecomateriales y Energía, Instituto de Ingeniería Civil
Facultad de Ingeniería Civil, Universidad Autónoma de Nuevo León
Cd. Universitaria, San Nicolás de los Garza, N. L. C. P. 66451
MÉXICO

²Division of Materials and Chemical Engineering
Sun Moon University
ChungNam 336-708
SOUTH KOREA

*Corresponding author: letorresg@yahoo.com, letorre@fic.uanl.mx

Abstract: - Pyrochlore-type structure compounds, Bi₂MTaO₇ (M = Al, Fe, Ga, In), were synthesized by both the sol-gel and solid state method. In order to evaluate their photocatalytic activity, these compounds were tested on the degradation reaction of alizarin red S, methyl orange and phenol in aqueous solution. The characterization of the compounds included: XRD, SEM/EDS, S_{BET} area, E_g value, DTA/TGA and FTIR. Pyrochlore-type structure compounds were obtained at lower temperatures (600-800°C) when they were prepared by the sol-gel method. The morphology of these compounds revealed the presence of nanoparticles. These materials also presented better S_{BET} values (from 58 to 11 m².g⁻¹) than those obtained by the solid state method (<5 m².g⁻¹). All the materials showed E_g values within the visible light region (2.2-1.3 eV). Iron-containing pyrochlore prepared by the sol-gel method had the best performance as photocatalyst under visible light conditions for alizarin red S degradation, and under UV-light for phenol degradation. The photocatalytic results suggested this tendency: Fe > In > Al > Ga for alizarin red s, and Fe > Ga > Al > In, for phenol degradation. In addition, the photocatalytic tests on alizarin red s and methyl orange under UV light showed the following tendency: In > Fe > Al > Ga. Best half time life ($t_{1/2}$) was obtained for alizarin red S degradation, ~30 min., using Bi₂InTaO₇ as photocatalyst, which was prepared by both the sol-gel method (at 600°C) and the solid state method (at 950°C). It seems that crystal structure has more influence than specific surface area for the organic compounds degradation carried out in this work.

Key-Words: Pyrochlore-type structure; Sol-gel; Photocatalytic performance; Degradation reaction; Alizarin red S.

1 Introduction

Environmental pollution is growing year by year, and quality of life is decreasing. Although there are several pollutant agents affecting the environment, water contamination and atmospheric pollution have been received more attention in order to increase quality of life [1-3]. Conventional technologies (biological, biochemical, physical process, and chemical processes) have been used to face water and atmospheric contamination, but they are not totally efficient to solve the environmental pollution problem. In that sense, alternative technologies, such as heterogeneous photocatalysis, are necessary to decrease environmental pollution more efficiently. Particularly, during the last decade, heterogeneous photocatalysis has been used as a great potential technology for the

degradation of hazardous organic pollutants, heavy metals removal, inactivation of microorganisms, and also for the water splitting reaction to obtain hydrogen as a clean energy source [4-9]. Several compounds have been prepared by different methods in order to develop new materials that can perform efficiently the redox reactions implicated in the photocatalysis process. In addition, these materials must be activated under visible light to have a sustainable process in waste water treatment or water splitting reaction. However, most of these materials are modifications of TiO₂ or titania-based oxides whose activities are still low [10-14]. Such a situation made a big role of the development of new semiconductor materials different from TiO₂ that could be activated under UV and visible light.

In this sense, pyrochlore materials ($A_2^{+3}B_4^{+2}O_7$) appear as alternative photocatalysts, where Bi_2MNbO_7 ($M = \text{Al, Ga, Fe or In}$) in particular has presented a higher photocatalytic activity in the water conversion reaction than TiO_2 , whose efficiency has been attributed to the charge mobility, which directly affects the properties of the semiconductor material [15-16]; and also in organic pollutant degradation, where their photocatalytic activity was mainly due to their textural properties because of the synthesis method, sol-gel [17-18].

Recently, Wang et al. reported a new series of pyrochlore materials: tantalate pyrochlores, Bi_2MTaO_7 ($M = \text{Fe, Ga or In}$); these compounds were synthesized by the solid state reaction and tested as photocatalyst materials on the water conversion reaction [19-21]. For this reason, in the present work, it was decided to carry out the synthesis of the pyrochlore materials with general formula Bi_2MTaO_7 ($M = \text{Al, Ga, Fe or In}$), but in order to improve their photocatalytic properties, these materials were synthesized by the sol-gel method. In addition, the results of their photocatalytic activity in the alizarin red S, methyl orange and phenol degradation are shown.

2 Experimental part

2.1 Synthesis

The pyrochlore-type structure materials were prepared by both the sol-gel and solid state reaction methods. Firstly, Bi_2MTaO_7 ($M = \text{Al, Ga, Fe or In}$) photocatalysts were synthesized by the sol-gel method following the methodology shown in Fig. 1.

All starting materials such as alcoxides were obtained from Aldrich (99.99%, Aldrich), whereas solvents like ethanol, acids and ammonium hydroxide were obtained from DEQ (99.8%).

After the fresh samples were obtained, some portions of these materials were calcined at different temperatures until reaching the maximum crystallization at 800°C ; the heating rate was $1^\circ\text{C}/\text{min}$.

On the other hand, the solid state preparation was carried out using oxides of the involved metals; the starting materials were obtained from Aldrich (99.99%), *i.e.* Bi_2O_3 , Ta_2O_5 , In_2O_3 and so on. These raw materials were mixed in stoichiometric amounts and calcined under air atmosphere at different temperatures and time conditions until reaching the maximum crystallization; the heating rate was $1^\circ\text{C}/\text{min}$.

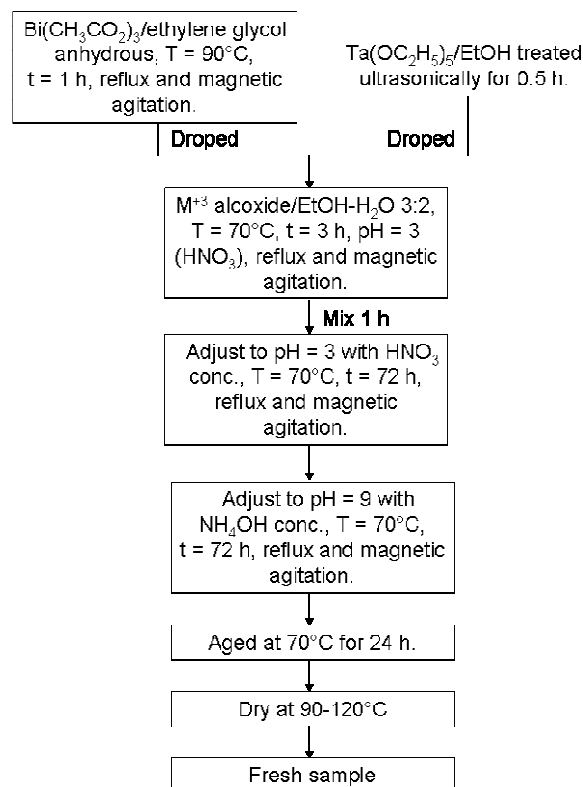


Fig. 1. Experimental diagram for the synthesis of pyrochlore compounds.

2.2 Structural characterization

The structure characterization was carried out by means of X-ray diffraction (XRD) using a Bruker D8 Advance diffractometer with $\text{CuK}\alpha$ radiation ($\lambda = 1.5418$); and scanning electron microscopy (SEM) using a JEOL JSM-6490-LV microscope coupled with X-ray energy dispersion (EDS).

2.3 Thermal evolution of fresh samples

The thermal evolution of sol-gel fresh samples was followed by means of thermo-gravimetric analysis (DTA/TGA) using a TA-Instruments SDT Q600 thermal analyzer in nitrogen flow, and infrared spectroscopy analysis (FTIR) using a Nicolet 360 spectrophotometer; wave number range of $4000\text{-}400\text{ cm}^{-1}$.

2.4 Photophysical and textural properties

The band gap energy value (E_g) was obtained from the UV spectra measured in a Perkin-Elmer Lambda 35 UV-vis spectrometer, whereas the specific surface area (S_{BET}) was determined by nitrogen physisorption at 77 K using a Quantachrome NOVA 2000e analyzer.

2.5 Photocatalytic degradation of alizarin red S, methyl orange and phenol under UV and visible light

The photocatalytic degradation of alizarin red S (ARS) and methyl orange was carried out using a hermetic quartz reactor. 200 mL of an aqueous solution of ARS or methyl orange (30 ppm) was prepared and then, 150 mg of Bi_2MTaO_7 powder ($M = \text{Al, Ga, Fe or In}$) were added to the reaction system under magnetic stirring and constant temperature. This solution was kept under dark conditions around 60 minutes to establish the reactant adsorption equilibrium. Then, two Pen-ray standard lamps were used as light sources, 4400 Mw.cm^{-2} at $\lambda = 254 \text{ nm}$ for UV-light and $\lambda = 365 \text{ nm}$ for visible-light. The degradation reaction was followed by means of UV spectra measurements considering the main absorption bands for each one of the dyes, in a Perkin-Elmer Lambda 35 UV-Vis spectrometer. Aliquots were collected at time intervals of 15-30 minutes for 4 h.

In the case of phenol degradation, it was used a continuous flux reactor with two canals connected to a recirculation system; flux was 35 mL/min . 50 mL of a phenol solution (100 ppm) was placed in each side of the canals of the system. 0.5 g of photocatalyst was distributed along the canal. Photocatalytic reactor was covered with plastic, and a UV lamp of $\sim 1600 \text{ mW.cm}^{-2}$ was used as irradiation source. After 60 min., for the absorption equilibrium, lamp was turn on. The degradation reaction was followed by means of UV spectra measurements in a Perkin-Elmer Lambda 35 UV-Vis spectrometer. Aliquots were collected at time intervals of 60 min., for 10 h [22].

3 Results and discussion

3.1 Synthesis and characterization of pyrochlore-type compounds

All the pyrochlore compounds were obtained by the sol-gel and solid state reaction methods; except $\text{Bi}_2\text{AlTaO}_7$, which was obtained only by the solid state reaction.

Fig. 2 shows the XRD pattern obtained for $\text{Bi}_2\text{GaTaO}_7$ synthesized by the sol-gel and solid state reaction method. The XRD patterns were compared with those previously reported by Wang et al. [20]; and good concordance between the patterns was observed.

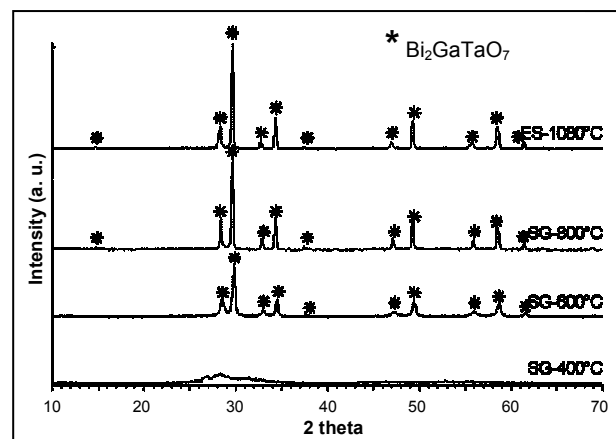


Fig. 2. XRD patterns of $\text{Bi}_2\text{GaTaO}_7$ prepared by sol-gel and solid state reaction.

In the case of the pyrochlores containing Fe, In and Al, the presence of the pyrochlore phase was mainly detected at 600 and 800°C, but the presence of a secondary phase in small proportion was also found. Table 1 shows a summary of the phases detected and identified by XRD.

Table 1. Summary of XRD characterization of the Bi_2MTaO_7 ($M = \text{Al, Fe, Ga or In}$) pyrochlore-type photocatalysts.

Material	Synthesis method	Thermal treatment (°C)	Identified phases
$\text{Bi}_2\text{AlTaO}_7$	sol-gel	400	$\text{Bi}_2\text{O}_3 + \text{Ta}_2\text{O}_5 + \text{Al}_2\text{O}_3 + \text{AlTaO}_4$
		600	$\text{Bi}_2\text{AlTaO}_7 + \text{Bi}_3\text{TaO}_7$
		800	$\text{Bi}_2\text{AlTaO}_7 + \text{Bi}_3\text{TaO}_7$
	solid state	725	$\text{Bi}_2\text{AlTaO}_7$
$\text{Bi}_2\text{FeTaO}_7$	sol-gel	400	Amorphous
		600	$\text{Bi}_2\text{FeTaO}_7$
		800	$\text{Bi}_2\text{FeTaO}_7 + \text{FeTaO}_4 + \text{Fe}_2\text{O}_3$
	solid state	1080	$\text{Bi}_2\text{FeTaO}_7 + \text{Fe}_2\text{O}_3$
$\text{Bi}_2\text{GaTaO}_7$	sol-gel	400	Amorphous
		600	$\text{Bi}_2\text{GaTaO}_7$
		800	$\text{Bi}_2\text{GaTaO}_7$
	solid state	1080	$\text{Bi}_2\text{GaTaO}_7$
$\text{Bi}_2\text{InTaO}_7$	sol-gel	400	$\text{Bi}_2\text{O}_3 + \text{In}_2\text{O}_3$
		600	$\text{Bi}_2\text{InTaO}_7 + \text{In}_2\text{O}_3$
		800	$\text{Bi}_2\text{InTaO}_7 + \text{In}_2\text{O}_3$
	solid state	950	$\text{Bi}_2\text{InTaO}_7 + \text{In}_2\text{O}_3$

It is important to emphasize that $\text{Bi}_2\text{AlTaO}_7$ was prepared by the first time by the solid state reaction and its presence was confirmed by using the $\text{Bi}_2\text{AlNbO}_7$ XRD pattern reported by Torres-Martinez, et al. [18], which is isostructural to this compound, see Fig. 3.

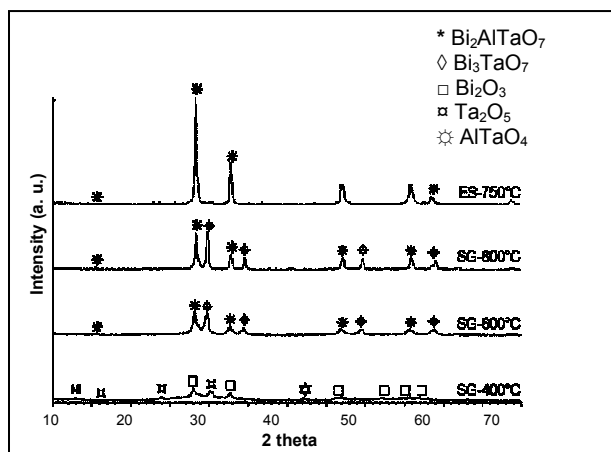


Fig. 3. XRD patterns of $\text{Bi}_2\text{AlTaO}_7$ prepared by sol-gel and solid state reaction.

Fig. 4 shows the micrographs of the pyrochlores prepared by both the sol-gel method at 600°C and solid state reaction. Pyrochlores containing Ga, In and Fe (Fig. 4a, 4b and 4c) prepared by sol-gel exhibited a heterogeneous morphology with particle size lower than $1\ \mu\text{m}$ (nanoparticles). In contrast, pyrochlore containing In and prepared by the solid state reaction at 950°C (Fig. 4d) clearly showed the presence of sintered particles.

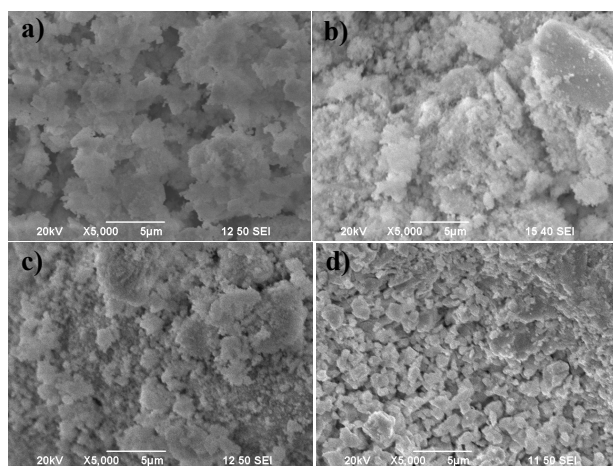


Fig. 4. SEM micrographs for pyrochlore compounds prepared by the sol-gel method at 600°C : a) $\text{Bi}_2\text{GaTaO}_7$, b) $\text{Bi}_2\text{InTaO}_7$, c) $\text{Bi}_2\text{FeTaO}_7$; and by the solid state reaction at 950°C : d) $\text{Bi}_2\text{InTaO}_7$.

3.2 DTA/TGA Analysis

Sol-gel fresh samples were analyzed by DTA/TGA analysis in order to follow their thermal evolution. Fig. 5 shows the thermogram for $\text{Bi}_2\text{InTaO}_7$ sample. It was observed at least five weight losses in the TGA curve before sample reaches its crystallization around 760°C . Firstly, 4% loss of the total mass was detected from 25 to 100°C (1).

This event was associated to desorption of adsorbed water and organic solvents (ethanol), as consequence, an endothermic process around 70°C was observed in DTA curve (A). From 100 to 200°C , a second weight loss ($\sim 5\%$) was detected (2), which was attributed to volatile organic matter and solvents elimination (ethylene glycol). This event was accompanied with an endothermic process at 180°C (B). Around 190°C it was observed the presence of an exothermic process, which could be associated with an oxidation process, phase crystallization, or chemical reaction; however oxidation is not possible because heating was conducted in nitrogen atmosphere. Probably a chemical reaction occurred between organic residual matters. Another weight loss (3) was detected from 200 to 260°C ($\sim 5\%$), which was related to the loss of coordinated water; endothermic process appears at 230°C (D). The fourth weight loss detected ($\sim 10\%$) was observed from 260 to 400°C (4). This event was attributed to decomposition of the residual organic matter. Two exothermic processes were observed, at 280°C (E) and 350°C (F). Above 400°C a slightly weight loss ($\sim 2\%$) was detected (5), corresponding to the sample dehydroxilation. This event was corroborated with the presence of an endothermic process around 730°C (G). Finally, around 760°C , the crystallization of the phase $\text{Bi}_2\text{InTaO}_7$ occurred; an exothermic process was detected (H).

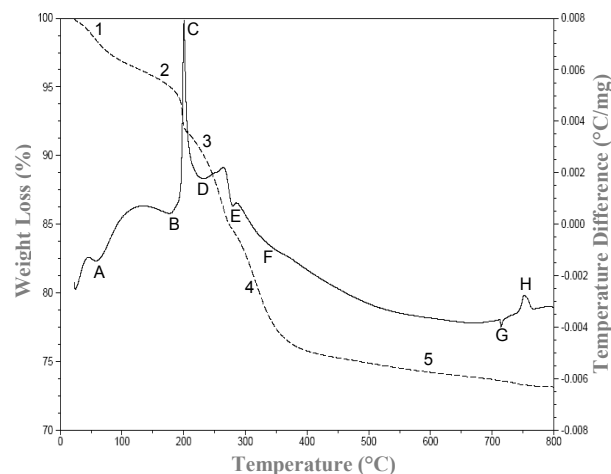


Fig. 5. DTA/TGA thermogram of sol-gel fresh sample for pyrochlore compound $\text{Bi}_2\text{InTaO}_7$.

3.3 FTIR Analysis

Fig. 6 shows FTIR spectra of pyrochlore compound, $\text{Bi}_2\text{InTaO}_7$, prepared by sol-gel. Fresh sample shows a wide absorption band at $3,500\ \text{cm}^{-1}$; its presence was related with the O-H bond from water adsorbed. In addition, flexions bands at $1,500$

cm^{-1} , and $1,400\text{-}1,250\text{ cm}^{-1}$ were detected, which were attributed to C-H bond, corresponding to $-\text{CH}_2$ and $-\text{CH}_3$ functional groups, respectively. Stretching band at $1,100\text{-}1,000\text{ cm}^{-1}$ corresponding to C-O bond was observed too. This band was related to primary alcohols such as ethanol and ethylene glycol, which were used for the sol-gel synthesis. On the other hand, as temperature increases, the majority of these bands disappeared. Above 600°C , only the vibration bands of M-O bond was detected below 700 cm^{-1} . This means that sol-gel sample is free of residual matter above this temperature. FTIR analysis detected the presence of water, organic solvents and organic matter in the fresh sample below 600°C , as it was observed by DTA/TGA analysis. Both analysis showed congruent results because also above 600°C it was detected just the M-O bond, corresponding to the presence of $\text{Bi}_2\text{InTaO}_7$.

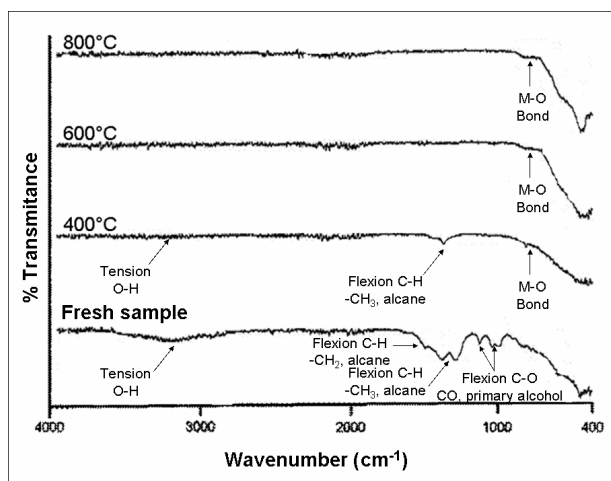


Fig. 6. FTIR spectra of sol-gel fresh sample for pyrochlore compound $\text{Bi}_2\text{InTaO}_7$.

3.4 Photophysical and textural properties

The E_g values of the pyrochlore compounds synthesized in this work were determined by UV-spectroscopy. Fig. 7 shows the UV spectra of each one of the pyrochlore compounds prepared by the solid state reaction.

It can be seen that all the compounds absorbed around $\lambda = 400\text{ nm}$. However, in the case of $\text{Bi}_2\text{FeTaO}_7$, two E_g values were determined at $\lambda = 400\text{-}600\text{ nm}$, and $\lambda = 600\text{-}800\text{ nm}$. Such a situation is due to the presence of two conduction bands, Ta_{5d} and Fe_{3d} .

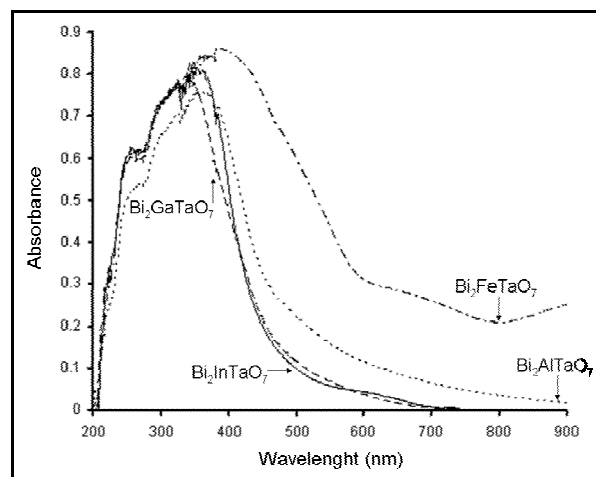


Fig. 7. UV-Vis spectra of solid state Bi_2MTaO_7 ($M = \text{Al, Ga, Fe or In}$).

In addition, it was determined that the E_g values of the pyrochlores synthesized by sol-gel were lower than the E_g values of the solid state compounds; all the materials showed E_g values within the visible light region ($2.2\text{-}1.3\text{ eV}$), see Table 2.

Table 2. S_{BET} and E_g values obtained from the Bi_2MTaO_7 ($M = \text{Al, Ga, Fe or In}$) materials.

Material	Synthesis method	Thermal treatment ($^\circ\text{C}$)	S_{BET} ($\text{m}^2\cdot\text{g}^{-1}$)	E_g value (eV)
$\text{Bi}_2\text{AlTaO}_7$	sol-gel	400	31	2.4
		600	16	2.1
		800	7	2.0
$\text{Bi}_2\text{FeTaO}_7$	solid state	725	< 5	2.5
		1080	< 5	1.8/2.4
$\text{Bi}_2\text{GaTaO}_7$	sol-gel	400	58	1.5
		600	17	1.4
		800	8	1.3/2.1
$\text{Bi}_2\text{InTaO}_7$	solid state	725	< 5	2.5
		1080	< 5	2.5
		950	< 5	2.7

According to this result, all the pyrochlore compounds could be activated under visible light for the degradation or alizarin red S; in particular the pyrochlore compound containing Fe because of its two conduction bands. Also, in Table 2 it is shown the S_{BET} values for the synthesized compounds.

It is observed that the S_{BET} values decrease when temperature increases; for this reason, all the materials synthesized by sol-gel and thermally treated at 600°C exhibited S_{BET} values 3 times

higher than those of the solid state compounds. According to the aforementioned, it is expected that the pyrochlore materials prepared by sol-gel show better performance in the photocatalytic degradation of alizarin red S.

3.5 Alizarin red S photodegradation under UV and visible light

In fig. 8 it is shown the behavior of ARS degradation under UV light.

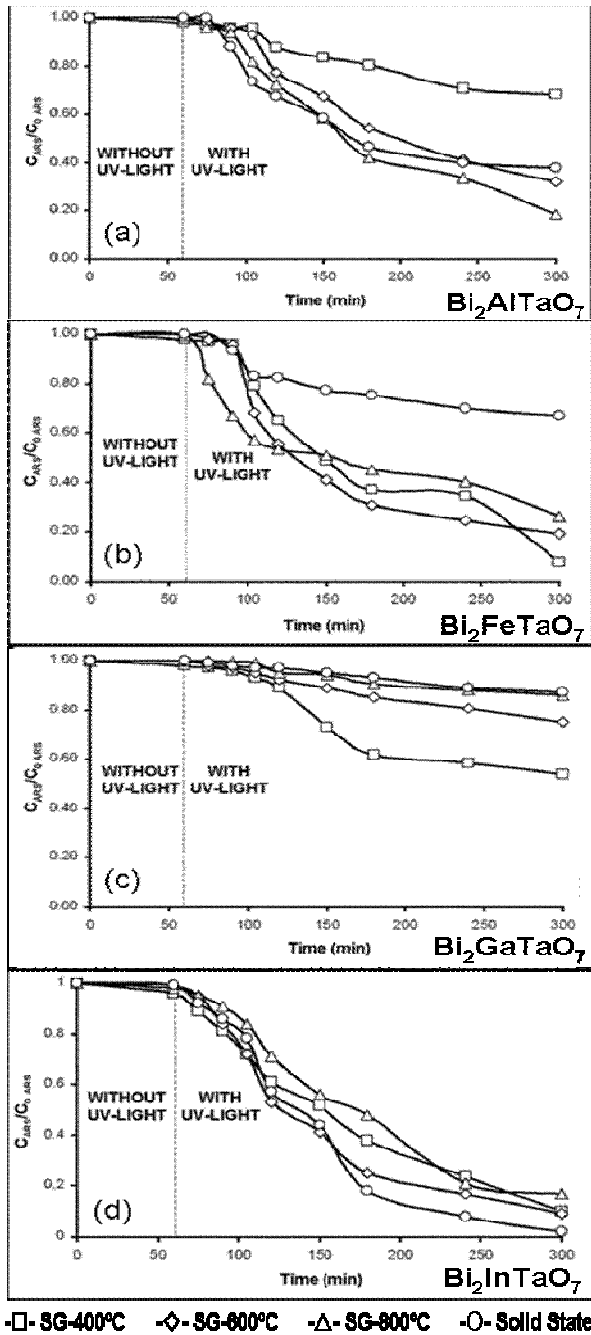


Fig. 8. Alizarin red S degradation using Bi_2MTaO_7 as photocatalyst under UV-light: (a) $\text{Bi}_2\text{AlTaO}_7$, (b) $\text{Bi}_2\text{FeTaO}_7$, (c) $\text{Bi}_2\text{GaTaO}_7$ and (d) $\text{Bi}_2\text{InTaO}_7$.

The Bi_2MTaO_7 ($M = \text{Al, Ga, Fe or In}$) compounds prepared by sol-gel and solid state reaction were tested as photocatalysts in the degradation reaction of alizarin red S under UV and visible light.

The highest ARS degradation was obtained when the pyrochlore containing In was used as photocatalyst; especially, the sample prepared by the sol-gel method at 600°C , and the sample synthesized by the solid state reaction at 950°C . In fact, it was determined that the tendency of the photocatalytic activity in the ARS degradation is as follows: $\text{In} > \text{Fe} > \text{Al} > \text{Ga}$.

In addition, it was found that the photocatalytic behavior of pyrochlore compounds used as photocatalysts on alizarin red S degradation follows a pseudo-first-order kinetic reaction model. Fig. 9 shows the kinetic curves for $\text{Bi}_2\text{InTaO}_7$ photocatalyst.

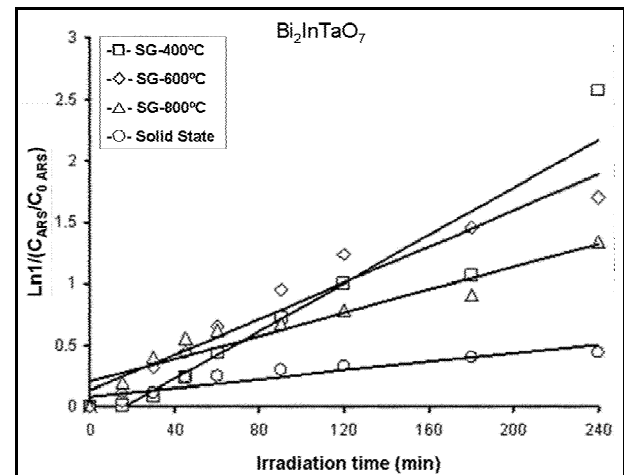


Fig. 9. Pseudo-first-order kinetic reaction of the pyrochlore $\text{Bi}_2\text{InTaO}_7$ on the alizarin red S degradation under UV light.

Using the information from the kinetic curves, it was determined the half time life ($t_{1/2}$) for each one of the pyrochlore compounds tested as photocatalysts on the alizarin red S degradation under UV light, see fig. 10. In this case, the best half time life ($t_{1/2}$) of the degradation reaction was obtained when $\text{Bi}_2\text{InTaO}_7$ was used as photocatalyst (~ 30 min.), which was prepared by both the sol-gel method (at 600°C) and the solid state method (at 950°C). It seems that pyrochlore compounds prepared by sol-gel showed the following tendency on the alizarin red S degradation under UV light: $\text{In} > \text{Fe} > \text{Al} > \text{Ga}$.

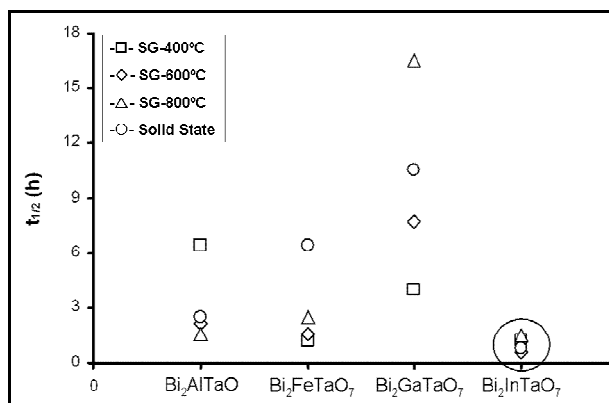


Fig. 10. Half time life ($t_{1/2}$) of the pyrochlore compounds on the alizarin red S degradation under UV light.

According to this information, it seems that the specific surface area has not enough influence on the photocatalytic performance of the ARS degradation. In this case, it seems that the crystal structure plays an important role in the photocatalytic activity.

This behavior could be explained also considering the M-O-M bond angles of the corner-linked MO_6 octahedral of Bi_2MTaO_7 ($M = \text{Fe}, \text{Ga}$ or In) compounds, as reported by Wang et al. [19], see Table 3. The photoinduced electrons and holes can move more easily if the angle between the corner-linked octahedral is closer to 180° , which affects the probability of electrons and holes to reach reaction sites on the catalyst surface. In this case, $\text{Bi}_2\text{InTaO}_7$ is the photocatalyst that has the M-O-M bond angle closer to 180° because it presents an ionic radius of 0.92 \AA , causing more distortion in the pyrochlore structure.

Table 3. M-O-M bond angles of the corner-linked MO_6 octahedral in the Bi_2MTaO_7 ($M = \text{Fe}, \text{Ga}$ or In) pyrochlore compounds [19].

Pyrochlore compounds	M-O-M angle ($^\circ$)	r_i (\AA)
$\text{Bi}_2\text{FeTaO}_7$	128.3	0.65
$\text{Bi}_2\text{GaTaO}_7$	134.6	0.62
$\text{Bi}_2\text{InTaO}_7$	143.4	0.92

On the other hand, the pyrochlore compounds were also tested as photocatalysts on the degradation of alizarin red S under visible light. The pyrochlore containing Fe, synthesized by the sol-gel method and thermally treated at 600°C , showed the best performance in the ARS degradation (20%). This result showed that $\text{Bi}_2\text{FeTaO}_7$ can be activated in the visible light region. In addition, the S_{BET} of the sol-gel material ($17 \text{ m}^2\cdot\text{g}^{-1}$) contributed to have a bigger contact area with ARS, making possible to carry out the photocatalytic process. Although the

photocatalytic performance under visible light is low, the results suggested the following tendency: $\text{Fe} > \text{In} > \text{Al} > \text{Ga}$.

Wang, et. al.[19] reported that although E_g values suggests the activation of pyrochlore compounds under visible light irradiation, generally it is necessary an energy higher than the E_g to maintain the charges mobility, giving the opportunity that transport phenomena occurs in the photocatalysts surface. In that way, this work uses the sol-gel method in order to improve the structure and physic-chemical properties of pyrochlore compounds. However photocatalytic results under visible light irradiation still are low. It is necessary to improve the photocatalytic activity of the studied pyrochlores under visible light irradiation by increasing the photocatalyst quantity, variations of the pH of the photocatalytic reaction, control of morphology, or adding an oxygen source to the reaction system.

3.6 Methyl orange photodegradation under UV and visible light irradiation

Photocatalytic results about the methyl orange photodegradation under UV light are showed in Table 4.

It is observed that best result of the degradation and half time life ($t_{1/2}$) for the photocatalytic reaction of methyl orange under UV-light irradiation was obtained using $\text{Bi}_2\text{InTaO}_7$ prepared by sol-gel and heat treated at 800°C . In general, the use of sol-gel method favors the photodegradation of this dye, which is showing the following tendency: $\text{In} > \text{Fe} > \text{Al} > \text{Ga}$.

Table 4. Photodegradation parameters for methyl orange under UV-light irradiation after 5 hours, using Bi_2MTaO_7 ($M = \text{Al}, \text{Fe}, \text{Ga}$ or In) pyrochlore compounds.

Synthesis	$\text{Bi}_2\text{AlTaO}_7$		$\text{Bi}_2\text{FeTaO}_7$		$\text{Bi}_2\text{GaTaO}_7$		$\text{Bi}_2\text{InTaO}_7$	
	%D	$t_{1/2}$ (h)						
SG-400	60	5.5	20	16.5	40	6.0	60	1.0
SG-600	40	5.0	50	5.0	50	4.0	60	0.5
SG-800	25	9.5	70	2.0	30	8.5	80	1.0
SS-1080*	40	2.5	55	3.0	40	5.5	60	0.5

*Sample synthesized by solid state reaction at 1080°C .

3.7 Phenol degradation under UV-light irradiation

All pyrochlore materials were tested as photocatalyst for the phenol degradation under UV-light irradiation. With exception of $\text{Bi}_2\text{FeTaO}_7$, all compounds showed less than 50% of phenol degradation after 10 hour of UV-light irradiation. Figure 11 shows the photocatalytic degradation of phenol using $\text{Bi}_2\text{FeTaO}_7$ as photocatalyst. It is observed that sol-gel sample at 800°C showed the highest photocatalytic performance. This behavior was attributed to the conduction bands present in this compound, Fe3d and Ta5d orbitals, where electron-hole pairs are easily generated.

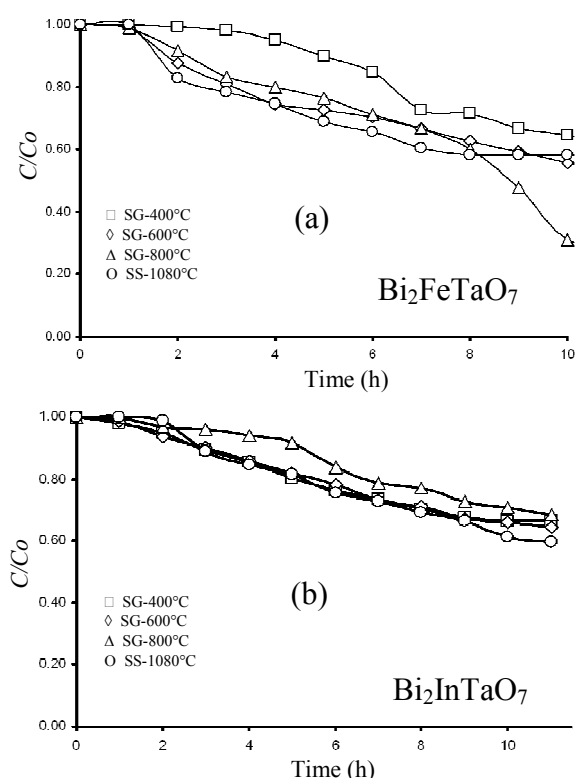


Fig. 11. Phenol photodegradation after 10 hours of UV-light irradiation using: (a) $\text{Bi}_2\text{FeTaO}_7$ and (b) $\text{Bi}_2\text{InTaO}_7$, as photocatalyst.

From photodegradation curves data it was calculated the kinetic parameters for phenol degradation using pyrochlore type compounds as photocatalysts, see table 5. According to these results, tendency of phenol degradation under UV-light irradiation is as follow: Fe>Ga>Al>In.

Table 5. Kinetic parameters for the phenol photodegradation using Bi_2MTaO_7 (M = Al, Fe, Ga, In) as photocatalysts under UV-light irradiation.

Synthesis T (°C)	$\text{Bi}_2\text{AlTaO}_7$		$\text{Bi}_2\text{FeTaO}_7$		$\text{Bi}_2\text{GaTaO}_7$		$\text{Bi}_2\text{InTaO}_7$	
	$t_{1/2}$ (h)	k (min^{-1})						
SG-400	14	0.0008	14	0.0008	13	0.0009	14	0.0008
SG-600	17	0.0011	11	0.0011	10	0.0011	14	0.0008
SG-800	12	0.0015	8	0.0015	10	0.0018	17	0.0006
Solid state	15	0.0011	10	0.0011	12	0.0011	14	0.0006

It is clear that for the photocatalytic degradation of phenol the process takes more time because of the complexity of the molecule, which is not easy to break.

According to the UV and visible light photocatalytic results, the pyrochlore compounds synthesized in this work showed their best efficiency under UV light. However in the case of the phenol photodegradation it seems that it is necessary more time because of the complexity to destroy the aromatic ring.

Although all materials showed E_g values within the visible region, it seems that it is necessary to use higher energy than the E_g values of the semiconductor materials to provoke the charge mobility in order to have a more active surface.

In all systems, it was observed that solid state compounds showed almost same behavior than sol-gel compounds (600 and 800°C), where crystal structure was formed. It seems that at least in this work, the crystal structure has more influence than the S_{BET} or E_g value for the photodegradation of alizarin red s, methyl orange and phenol.

In addition, other factors such as: solution pH change, control of particle morphology and addition of an oxygen source to the reaction system could increase the photocatalytic performance under visible light irradiation.

4 Conclusions

Pyrochlore-type structure compounds, Bi_2MTaO_7 (M = Al, Ga, Fe or In), were synthesized by the sol-gel method at lower temperatures than those obtained by the solid state reaction. In addition, $\text{Bi}_2\text{AlTaO}_7$ was prepared by the first time by the solid state reaction. These compounds showed the presence of the pyrochlore phase and a heterogeneous morphology with nanometric particle sizes. The textural and photophysical properties were enhanced by the synthesis method;

the S_{BET} values were 3 times higher than those obtained by the solid state reaction; and the energy band gap values were within the visible light region. The sol-gel pyrochlore compounds (600 and 800°C, where crystal structure was formed) showed the best performance as photocatalysts under UV (Tendency: In > Fe > Al > Ga), and visible light (Tendency: Fe > In > Al > Ga) conditions, but also solid state compounds showed almost same behavior. From all systems, the best photocatalytic performance was obtained using Bi₂InTaO₇ photocatalyst, synthesized by both the sol-gel and the solid state method, half time life ($t_{1/2}$) was ~30 min. It seems that at least in this work, the crystal structure has more influence than the specific surface area or E_g value on the alizarin red s, methyl orange and phenol degradation.

Acknowledgements

The authors want to thank CONACYT-Mexico and KRF-Korea for the economical support to the bilateral project between these nations from 2007 to 2009.

References

- [1] Quartieri J., Troisi A., Guarnaccia C., D'Agostino P., D'Ambrosio S., Iannone G., Development of an Environmental Quality Index Related to Polluting Agents, Proceedings of the 7th WSEAS International Conference on Environment, Ecosystems and Development (EED'09), 2009, pp. 153-161.
- [2] Ehsanollah Moosavi, Varsik Martirosyan, Sinerik Ayrapetyan, a new approach for water purification from microbial pollution, Proceedings of the 2nd International Conference on Environmental and Geological Science and Engineering (EG'09), 2009, pp. 38-43.
- [3] Tarek M. Abdel-Fattah, Nanomaterials for Water and Environmental Remediation, Proceedings of the 6th WSEAS International Conference on Environment, Ecosystems and Development (EED'08), 2008, pp. 106-109.
- [4] Sampa Chakrabarti, Basab Chaudhuri, Sekhar Bhattacharjee, On the removal of hexavalent chromium from wastewater: a comparative study between photocatalytic and chemical reduction processes, Proceedings of the 6th WSEAS International Conference on Environment, Ecosystems and Development (EED'08), 2008, pp. 32-37.
- [5] Gaya, U. I., Abdullah, A. H., Heterogeneous photocatalytic degradation of organic contaminants over titanium dioxide: A review of fundamentals, progress and problems, *Journal of Photochemistry and Photobiology C: Photochemistry Reviews*, Vol. 9, No. 1, 2008, pp. 1-12.
- [6] Augugliaro, V., Litter, M., Palmisano, L., Soria, J., The combination of heterogeneous photocatalysis with chemical and physical operations: A tool for improving the photoprocess performance, *Journal of Photochemistry and Photobiology C: Photochemistry Reviews*, No. 7, 2006, pp. 127-144.
- [7] Kudo, A., Development of photocatalyst materials for water splitting, *International Journal of Hydrogen Energy*, Vol. 31, No. 2, 2006, pp. 197-202.
- [8] Sun, B., Reddy, E. P., Smirniotis, P. G., Visible light Cr (VI) reduction and organic chemical oxidation by TiO₂ Photocatalysis, *Environmental Science Technology*, No. 39, 2005, pp. 6251-6259.
- [9] Zou, Z. Ye, J., Sayama, K., Arakawa, H., Direct splitting of water under visible light irradiation with an oxide semiconductor photocatalyst, *Nature*, No. 414, 2001, pp. 625-627.
- [10] Lachheb, H., Puzenat, E., Houas, A., Ksibi, M., Elaloui, E., Guillard, C., Herrmann, J. M., Photocatalytic degradation of various types of dyes (Alizarin S, Crocein Orange G, Methyl Red, Congo Red, Methylene Blue) in water by UV-irradiated titania, *Applied Catalysis B: Environmental*, Vol. 39, No. 8, 2002, pp. 75-90.
- [11] Oyama, T., Aoshima, A., Horikoshi, S., Hidaka, H., Zhao, J., Serpone, N., Solar Photocatalysis, photodegradation of a commercial detergent in aqueous TiO₂ dispersions under sunlight irradiation, *Fuel and Energy Abstracts*, Vol. 46, 2008, pp. 338.
- [12] Peng, F., Cai, L., Huang, L., Yu, H., Wang, H., Preparation of nitrogen-doped titanium dioxide with visible-light photocatalytic activity using a facile hydrothermal method, *Journal of Physical and Chemistry of Solids*, Vol. 69, No. 7, 2008, pp. 1657-1666.
- [13] Liu, Y., Wang, X., Yang, F., Yang, X., Excellent antimicrobial properties of mesoporous anatase TiO₂ and Ag/TiO₂ composite films, *Microporous and Mesoporous Materials*, Vol. 114, No. 1-3, 2008, pp. 431-435.
- [14] S.N. Hosseini, M. Borghei, M. Vossoughi, N. Taghavinia., Photocatalytic degradation of

- phenol in aqueous phase with TiO_2 immobilized on three different supports with a simple method, 3rd IASME/WSEAS Int. Conf. on Energy & Environment, University of Cambridge, UK, February 23-25, 2008.
- [15] Zou, Z., Ye, J., Arakawa, H., Photocatalytic and photophysical properties of a novel series of solid photocatalysts Bi_2MNbO_7 ($\text{M} = \text{Al}^{+3}$, Ga^{+3} , In^{+3}), *Chemical Physics Letters*, Vol. 333, No. 1-2, 2001, pp. 57-62.
- [16] Zou, Z., Ye, J., Arakawa, H., Photocatalytic decomposition of water with $\text{Bi}_2\text{InNbO}_7$; *Catalysis Letters*, Vol. 68, No. 3-4, 2000, pp. 235-239.
- [17] Garza-Tovar, L. L., Torres-Martínez, L. M., Bernal-Rodríguez, D., Gómez, R., del Ángel, G., Photocatalytic degradation of methylene blue on Bi_2MNbO_7 ($\text{M} = \text{Al}$, Fe , In , Sm) Sol-Gel catalysts, *Journal of Molecular Catalysis A: Chemical*, Vol. 247, 2006, pp. 283-290.
- [18] Garza-Tovar, L. L., Torres-Martínez, L. M., Bernal-Rodríguez, D., Treviño, N. N., Sol-Gel synthesis and photocatalytic properties of Bi_2MNbO_7 ($\text{M} = \text{Al}$, Fe , In , Sm), *Materials Science Forum*, Vol. 486/487, 2005, pp. 85-88.
- [19] Wang, J., Zou, Z., Jinhua, Y., Surface modification and photocatalytic activity of distorted pyrochlore-type Bi_2M ($\text{M} = \text{In}$, Ga and Fe) TaO_7 photocatalysts, *Journal of Physics and Chemistry of Solids*, No. 66, 2005, pp. 349-355.
- [20] Wang, J., Zou, Z., Ye, J., Synthesis, structure and photocatalytic property of a new hydrogen evolving photocatalysts $\text{Bi}_2\text{InTaO}_7$, *Functionally Graded Materials VII*, 2005, pp. 485-490.
- [21] Luan, J., Zou, Z., Lu, M., Zheng, S., Chen, Y., Growth, structural and photophysical properties of $\text{Bi}_2\text{GaTaO}_7$, *Journal of Crystal Growth*, Vol. 273, 2004, pp. 241-247.
- [22] Aguilar-Elguezabal, A., de la Cruz-Romero, D.; (2007); "Medición de la actividad fotocatalítica del TiO_2 dopado con tierras raras, Ce, La, Pr, y Nd en la degradación del fenol"; 3er Verano de Investigación Científica; Centro de Investigación en Materiales Avanzados, S. C.